Performance of DS-CDMA Over Measured Indoor Radio Channels Using Random Orthogonal Codes

Mitchell Chase, *Member, IEEE,* and Kaveh Pahlavan, *Senior Member, IEEE,*

Abstract—**Direct sequence spread spectrum, with its inherent resistance to multipath interference, has become a commercial reality for indoor wireless communications and has been proposed for personal communication networks. To allow multiple users within the limited bandwidths allocated by the FCC, code-division multiple-access (CDMA) is needed. This paper analyzes the performance of CDMA systems using random orthogonal codes over fading multipath indoor radio channels using channel measurements from five different buildings. The effect of RAKE receiver structure is studied, as is the effect of average power control. The average probability of error as a function of signal-to-noise ratio is used as the performance criteria. Results are compared with models for Rayleigh fading channels.**

I. Introduction

THE increasing popularity of portable personal communications has created a need for solutions to the interference and poor reception quality caused by the limited frequencies available and the close proximity of multiple users. One radio frequency (RF) technique already in commercial use for wireless indoor communications [1] is being investigated for portable personal communications. Direct sequence code-division multiple-access (DS-CDMA) communications offer an alternative to conventional RF indoor communications [2]. Spread spectrum provides resistance to the multipath caused by walls, ceilings, and other objects between the transmitter and receiver. Spread spectrum can overlay existing systems because of the low spectral density level. In the U.S. the FCC has assigned three bands for nongovernmental applications of spread spectrum which enhance this alternative for indoor channels [3]. The only reservation concerning DS-CDMA communications is the efficiency of the bandwidth utilization in fading multipath channels [4]. Coding and diversity combining can improve the bandwidth efficiency of DS-CDMA communications [5]–[7]. Diversity can be external (i.e., multiple antennas) or implicit (internal). Implicit diversity combining makes use of the inherent diversity from multipath reception and can be achieved with a RAKE receiver. Combinations of implicit and external diversities can be used to improve performance.

The performance of a system that transmits alternating sequences to minimize intersymbol interference with a multipath combining receiver over statistically modeled channels was considered in [8]. Another method for improving the bandwidth efficiency is the use of M-ary signaling. The bandwidth efficiency of M-ary orthogonal codes over nonfading channels is discussed in [9], and over fading channels in [10]. This paper analyzes such a system using measured multipath fading channel data. The particular examples use the measured multipath characteristics from five manufacturing areas [11] and a bandwidth permitted by the FCC [3]. A RAKE receiver structure is investigated and compared with theoretical results for Rayleigh fading channels.

Manuscript received November 30, 1992; revised March 26, 1993.
M. Chase is with Comdisco Systems, Inc., Natick, MA 01760.
K. Pahlavan is with Worcester Polytechnic Institute, Worcester, MA.
IEEE Log Number 9211017.

II. System Model

A. Transmitter:

The system (Fig. 1) [9] consists of K users, each assigned a set of sequences $V^{(k)}$ consisting of M-ary orthogonal sequences, each of length N;

$$V^{(k)} = \{V_1^{(k)}, V_2^{(k)}, \cdots, V_M^{(k)}\} \tag{1}$$

where

$$V_\lambda^{(k)} = \{V_{\lambda,0}^{(k)}, V_{\lambda,1}^{(k)}, \cdots, V_{\lambda,N-1}^{(k)}\} \tag{2}$$

and $V_{\lambda,n}^{(k)} = \exp(j\Theta_{\lambda,n}^{(k)})$ is a complex rth root of unity (r-phase modulation). M-ary equally likely data symbols are transmitted at a rate of one every T seconds. The complex envelope of the signal transmitted by the kth user to send the λ th symbol during the period $[0, T)$ is

$$X_k(V_\lambda^{(k)}, t) = A\tilde{X}_k(V_\lambda^{(k)}, t) \tag{3}$$

where

$$\tilde{X}_k(V_\lambda^{(k)}, t) = \sum_{n=0}^{N-1} V_{\lambda,n}^{(k)} P_{T_c}(t - nT_c - \Delta_k)\exp(j\theta_k) \tag{4}$$

and A is the amplitude of the transmitted signal. The chip duration T_c is $1/W$, W being the available bandwidth. P_{T_c} is the chip waveform, θ_k the carrier phase, and Δ_k represents the asynchronous transmission delay time between transmitters. Δ_k for $k \neq 0$ is uniformly distributed in $[0, T_c)$ with $\Delta_0 = 0$, and θ_k is uniformly distributed in $[0, 2\pi)$. The chip waveform is defined for $0 \leq t < T_c$, is zero outside the range, and is normalized so that the energy per chip is equal to T_c.

The overall transmitted signal for the kth user is

$$U_k(t) = \sum_{s=-\infty}^{\infty} X_k(V_m^{(k)}, t - sT); \qquad m = 1, 2, \cdots, M. \tag{5}$$

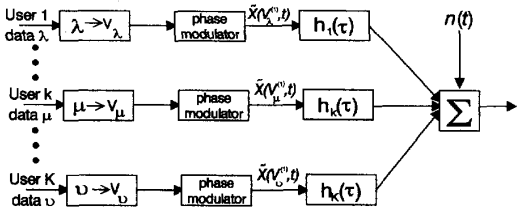

Fig. 1. System block diagram.

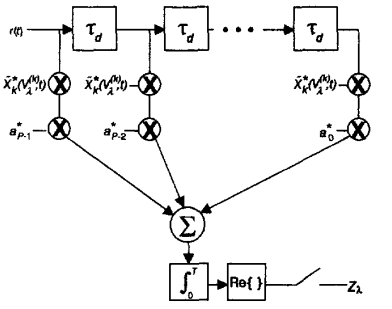

Fig. 2. RAKE receiver with maximal ration combining for the kth user and the λth symbol.

B. Channel:

The fading multipath indoor channels are assumed to be discrete and time-invariant with channel impulse response for each user given by [11]:

$$h_k(\tau) = \sum_{l=0}^{L_k-1} \alpha_l^{(k)} \delta(\tau - \tau_l^{(k)}) \exp(j\phi_1^{(k)}) \tag{6}$$

where $\alpha_l^{(k)}$, $\tau_l^{(k)}$, and $\phi_1^{(k)}$ are the path gain, delay and phase, respectively, $\delta(t)$ is the unit impulse function, and L_k is the number of multipaths for profile k. The path gain and delay for each channel are determined from actual measurements [11]. The path phase $\phi_l^{(k)} = 2\pi f_c \tau_l^{(k)}$ is assumed to be a uniformly distributed random variable in $[0, 2\pi)$ incorporating the carrier phase θ_k. The received signal is

$$r(t) = \sum_{k=0}^{K-1} \sum_{l=0}^{L_k-1} \alpha_l^{(k)} \exp(j\phi_l^{(k)}) U_k(t - \tau_l^{(k)}) + n(t) \tag{7}$$

where

$$n(t) = n_r(t) + jn_i(t); \qquad j = \sqrt{-1} \tag{8}$$

$n(t)$ is AWGN with power spectral density N_0.

C. Receiver:

To combat the multipath distortion and achieve better performance, diversity combining is needed [7]. A matched filter receiver structure is investigated that takes advantage of the implicit diversity of the received signal.

III. Receiver Structure

A. RAKE Receiver:

The optimum receiver for wideband fading multipath signals is a RAKE matched filter [12]. This receiver takes advantage of the implicit diversity of the multipaths in the received signal. Consider the coherent RAKE matched filter with maximal-ratio combining structure as shown in Fig. 2. The decision variable, Z_λ, for the first user and the λ th symbol is (Appendix A):

$$Z_\lambda = \mathrm{Re}\left\{ A \sum_{p=0}^{P-1} a_p \exp(-j\varphi_p) \sum_{k=0}^{K-1} \sum_{l=0}^{L_k-1} \alpha_l^{(k)} \exp(j\phi_l^{(k)}) \cdot \sum_{s=-\infty}^{\infty} R_{\nu,\lambda}^{(k,1)}\left(\tau_l^{(k)} - \frac{p}{W} + \Delta_k + sT\right) \right\} + \eta_\lambda \tag{9}$$

The receiver for M-ary signaling is shown in Fig. 3. The distribution of the correlation function $R_{\nu,\lambda}^{(k,1)}(\cdot)$ is approximately Gaussian by the central limit theorem. Similarly, the statistics of the difference of decision variables are assumed to follow a Gaussian distribution. Thus the probability of error can be expressed as

$$\Pr(\epsilon) \approx \frac{M-1}{2} \operatorname{erfc}\left(\sqrt{\frac{\gamma}{2}}\right). \tag{10}$$

. The energy per bit is

$$E_b = \frac{A^2}{2} \frac{NT_C}{\log_2 M}. \tag{11}$$

Hence, γ can be written as

$$\gamma = \gamma_{\mathrm{RAKE}} = \frac{\left[\sum_{p=0}^{P-1} \sum_{l=0}^{L_1-1} a_p \alpha_l^{(1)} \cos(\phi_l^{(1)} - \varphi_p) R_{\lambda,\lambda}^{(1,1)}\left(\tau_l^{(1)} - \frac{p}{W}\right)\right]^2}{\Omega_{\mathrm{RAKE}}} \tag{12}$$

for the RAKE receiver and

$$\begin{aligned}\Omega_{\mathrm{RAKE}} &= \sum_{p=0}^{P-1} \sum_{l=0}^{L_1-1} [a_p \alpha_l^{(1)} \cos(\phi_l^{(1)} - \varphi_p)]^2 Y_a\left(\tau_l^{(1)} - \frac{p}{W}\right) \\ &\quad + \sum_{k=1}^{K-1} \sum_{p=0}^{P-1} \sum_{l=0}^{L_k-1} [a_p \alpha_l^{(k)} \cos(\phi_l^{(k)} - \varphi_p)]^2 Y_b\left(\tau_l^{(k)} - \frac{p}{W}\right) \\ &\quad + \frac{N_0}{E_b} \frac{(NT_c)^2}{\log_2 M} \sum_{p=0}^{P-1} |a_p|^2 \end{aligned} \tag{13}$$

where $Y_a(\cdot)$ and $Y_b(\cdot)$ are related to the auto- and cross-correlation functions of the transmitted sequences (Appendix B). The first term represents the self-interference, the second term interference from other users, and the last term is noise.

B. Predicted Results:

The results of the simulations are compared with the theoretical performance for coherent detection of BFSK in fading channels [12]

$$\Pr(\epsilon) = \frac{1}{2}\left[1 - \sqrt{\frac{\overline{\gamma}}{2+\overline{\gamma}}}\right] \tag{14}$$

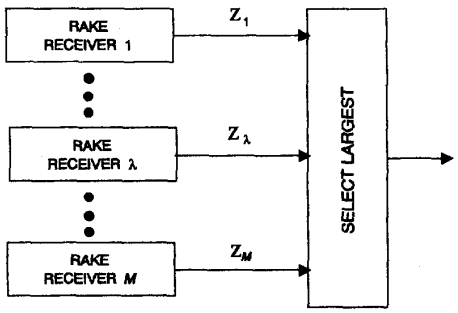

Fig. 3. M-ary RAKE receiver structure.

where the average signal-to-noise ratio is defined as

$$\overline{\gamma} = \frac{E_b}{N_0} E(a^2). \tag{15}$$

When diversity combining techniques are employed, the predicted performance for coherent detection of BFSK is [12]

$$\Pr(\epsilon) = \left(\frac{1-\mu}{2}\right)^L \sum_{k=0}^{L-1} \binom{L-1+k}{k} \left(\frac{1+\mu}{2}\right)^k \tag{16}$$

where

$$\mu = \sqrt{\frac{\overline{\gamma}}{2+\overline{\gamma}}} \tag{17}$$

and L is the order of diversity.

IV. Channel Measurements

A. Simulated

To confirm the validity of the system model and simulation program, two sets of computer generated channel profiles were used. The first set simulated a Rayleigh fading channel with one received path at $t = 0$. In the second set, each channel was assigned two path gains, one each at delays of $t = 0$ and $t = 1/W$. The path delay and tap spacing are ideal, thus allowing comparison with the expression of performance for fading channels (14). The amplitudes followed a Rayleigh distribution [6] with the parameter $\rho = 0.637$ and $E\{f(x)\} = 1.0$:

$$f(x) = \begin{cases} \frac{x}{\rho} \exp\left(-\frac{x^2}{2\rho}\right); & x \geq 0 \\ 0; & x < 0 \end{cases}. \tag{18}$$

B. Measured Channel Data:

Channel measurements were made at five different locations [10]. An RF oscillator on a mobile transmitter was used to generate a 910-MHz signal modulated by a train of 3-ns pulses with a 500-ns repetition period. The stationary base equipment comprised the receiver coupled to a digital storage scope and a personal computer. Both the transmitter and the receiver used vertically polarized quarter-wave dipole antennas placed about 1.5 m above floor level. The transmitter was moved to various locations in the site, and the received multipath profiles were stored in the computer. Each profile was an average of 64 channel snapshots collected in a 15 to 20-second period. The distance between the transmitter and the receiver varied between 1 and 50 meters. A total of about 300 profiles were collected from measurements made in five areas on three different manufacturing floors. The channel data represents a snapshot in time, providing an estimate of the performance, albeit at a particular time and location.

TABLE I
Multipath Statistics of the Five Measured Buildings

Area	RMS Multipath Delay Spread (ns)		
	Mean	Median	Maximum
A	16.6	15.25	40
B	29.0	31.62	60
C	73.1	52.57	150
D	33.1	19.37	146
E	52.4	48.90	152

Area A[1] with 54 profiles was a typical electronics shop floor having circuit board design equipment, soldering and chip mounting stations. Area B[2] with 48 profiles included test equipment and storage areas for common electronic equipment, partitioned by metallic screens. Area C[3] with 45 profiles was an automobile assembly line "jungle" comprising all kinds of welding and body shop equipment. Area D[4] with 66 profiles was a vast open area used for final inspection of the new cars coming off of the assembly line. Area E[5] with 75 profiles had grinding machines, huge ovens, transformers, and other heavy machinery. The multipath statistics of the five areas are shown in Table I.

V. Results and Discussion

The receiver analysis for one user with $M = 2$ and $N = 256$ over one- and two-path simulated Rayleigh fading channels is shown in Fig. 4. A one-tap coherent RAKE receiver was analyzed for the single path profiles, and a two-tap model for the two-path profiles. Simulations from 50000 computer generated channel profiles for each case were averaged and compared with the predicted results. The signal energies were adjusted for the profiles and the predicted results such that $E\{\alpha^2\} = 1.28$. The results for both one- and two-path models closely agree with predicted results until $\Pr(\epsilon) \approx 10^{-5}$, where errors due to machine underflow start to appear.

The effect of a RAKE receiver synchronized to the first received path is shown in Fig. 5. The performance over one of the measured areas (Area A) with various combinations of tap spacing and tap length is shown for the case of one active transmitter ($K = 1$, $M = 2$, $N = 256$, and 25 MHz bandwidth). Increasing receiver complexity by reducing tap spacing while adding more taps yields diminishing returns after the implicit diversity from the channel is realized by the receiver.

The performance of one active transmitter over all of the measured areas is shown in Fig. 6 ($K = 1$, $M = 2$, $N = 256$, and $W = 25$ MHz). A RAKE receiver synchronized to the

[1] Infinet Inc., N. Andover, MA
[2] Infinet Inc., N. Andover, MA
[3] General Motors, Framingham, MA
[4] General Motors, Framingham, MA
[5] Norton Company, Worcester, MA

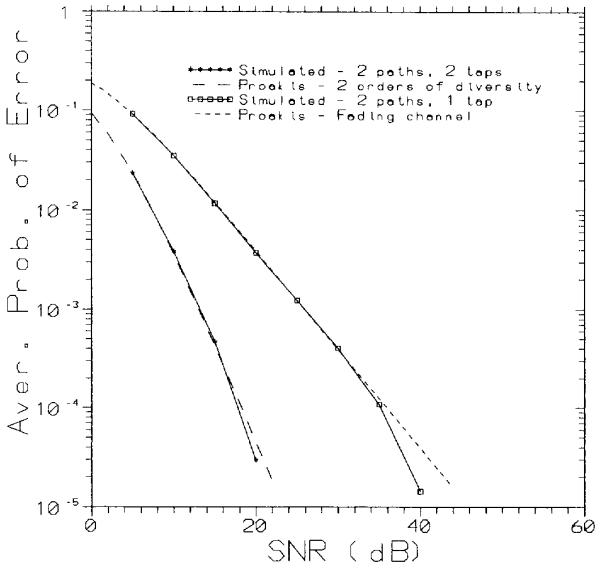

Fig. 4. Performance over Rayleigh simulated channel compared with predicted results.

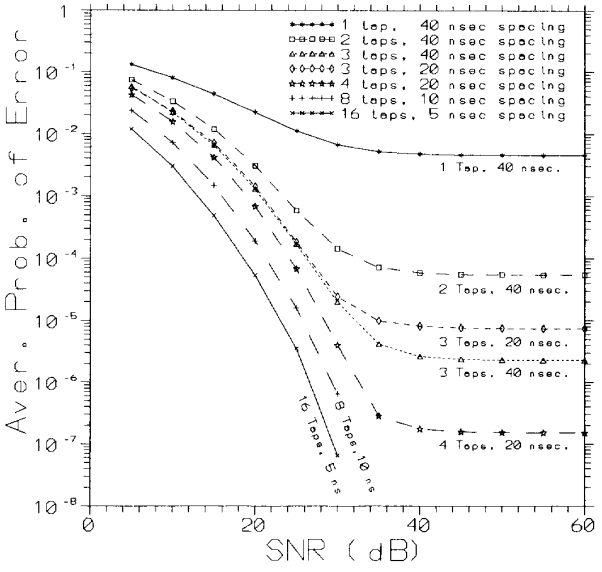

Fig. 5. Performance over Area A with one active transmitter using RAKE receivers of various combinations of tap spacing and tap length ($K = 1$, $M = 2$, $N = 256$, $W = 25$ MHz, no power control).

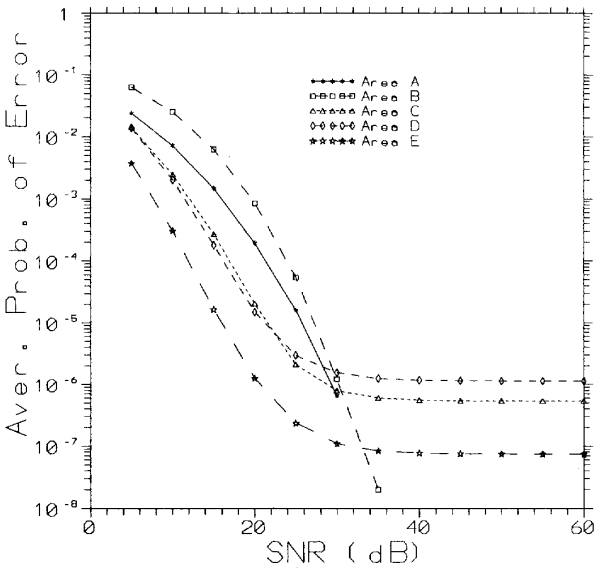

Fig. 6. Performance over measured area with one active transmitter using an 8-tap RAKE receiver with 10 ns tap spacing ($K = 1$, $M = 2$, $N = 256$, $W = 25$ MHz, no power control).

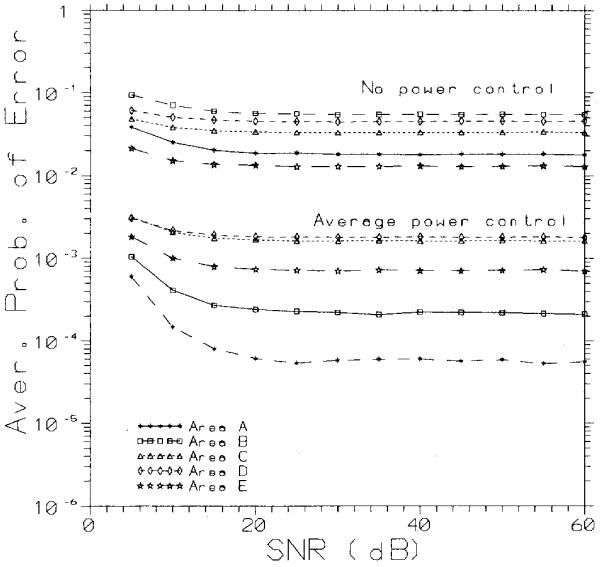

Fig. 7. Performance over measured channels with five active transmitters with and without power control using an 8-tap RAKE receiver with 10 ns tap spacing ($K = 5$, $M = 2$, $N = 256$, $W = 25$ MHz).

first received path with eight taps spaced 10 ns apart was utilized. Areas B, C, and D initially show better performance with this receiver until approximately 30 dB. The receiver structure chosen does not realize the implicit diversity inherent in those areas with higher multipath delay spread. Additional taps would be necessary to achieve the performance possible over these channels. The performance over Areas A and B is initially limited by the nature of the channels—metallic partitions and other structures limiting performance at lower signal energies.

The degradation of performance in multi-user systems is shown in Fig. 7. The same receiver as used in Fig. 5 is employed. The results without power control are uniformly poor. When the average energy of each *profile* from each area of the channel impulse response is normalized to unity, the performance improves by up to a factor of approximately 100. The effect is more pronounced in the areas with metallic partitions (Areas A and B) than in the other areas. The performance is related to the RAKE receiver structure and the multipath spread.

VI. Conclusions

The performance over indoor channels is highly dependent on the channel characterization as well as the receiver structure. Generalizations about the channel response will result in approximate results that may not be suitable for performance determinations without further study.

CDMA is an attractive solution to the problems encountered in portable personal communications. In addition to the attractions of spread spectrum, CDMA allows multiple users to share limited bandwidth. The traditional assumption of Rayleigh distributed fading multipath channels is not necessarily appropriate for the indoor radio channel. It is also apparent that each channel profile results in different received power levels. Uniform power assumptions for transmitter-receiver paths cannot be used. Power control is necessary for a multi-user system.

Appendix A
RAKE Receiver with Maximal Ratio Combining

The multiple-user M-ary received signal is

$$r(t) = \sum_{k=0}^{K-1} \sum_{l=0}^{L_k-1} \alpha_l^{(k)} \exp(j\phi_l^{(k)}) U_k(t - \tau_l^{(k)}) + n(t) \quad \text{(A1)}$$

where K is the number of simultaneous active transmitters, L_k is the number of multipaths received from the kth user and $\alpha_l^{(k)}$, $\tau_l^{(k)}$, and $\phi_l^{(k)}$ are the path gain, delay, and phase, respectively.

The decision variable for a RAKE receiver with maximal ratio combining for the first user and the λth symbol is (A2) and (A3), .

$$Z_\lambda = \mathrm{Re}\left\{ \int_0^T \sum_{p=0}^{P-1} a_p \exp(-j\varphi_p) \tilde{X}_1^*\left(V_\lambda^{(1)}, t - \frac{p}{W}\right) r(t)\, dt \right\} \quad \text{(A2)}$$

$$Z_\lambda = \mathrm{Re}\left\{ \sum_{p=0}^{P-1} a_p \exp(-j\varphi_p) \sum_{k=0}^{K-1} \sum_{l=0}^{L_k-1} \alpha_l^{(k)} \cdot \exp(j\phi_l^{(k)}) \int_0^T \tilde{X}_1^*\left(V_\lambda^{(1)}, t - \frac{p}{W}\right) U_k\left(t - \tau_l^{(k)}\right) dt \right\} + \mathrm{Re}\left\{ \sum_{p=0}^{P-1} \alpha_p \exp(-j\varphi_p) \int_0^T \tilde{X}_1^*\left(V_\lambda^{(1)}, t - \frac{p}{W}\right) n(t)\, dt \right\} \quad \text{(A3)}$$

Let

$$\eta_\lambda = \mathrm{Re}\left\{ \sum_{p=0}^{P-1} a_p \exp(-j\varphi_p) \cdot \int_0^T \tilde{X}_1^*\left(V_\lambda^{(1)}, t - \frac{p}{W}\right) n(t)\, dt \right\}. \quad \text{(A4)}$$

Then, expanding $U_k(t - \tau_l^{(k)})$ the decision variable becomes

$$Z_\lambda = \mathrm{Re}\left\{ \sum_{p=0}^{P-1} \alpha_p \exp(-j\varphi_p) \sum_{k=0}^{K-1} \sum_{l=0}^{L_k-1} a_l^{(k)} \exp(j\phi_l^{(k)}) \cdot \int_0^T \tilde{X}_1^*\left(V_\lambda^{(1)}, t - \frac{p}{W}\right) \cdot \sum_{s=-\infty}^{\infty} X_k(V_\nu^{(k)}, t - \tau_l^{(k)} - sT)\, dt \right\} + \eta_\lambda. \quad \text{(A5)}$$

Looking at the integral in (A5),

$$I = \int_0^T \tilde{X}_1^*\left(V_\lambda^{(1)}, t - \frac{p}{W}\right) \sum_{s=-\infty}^{\infty} X_k(V_\nu^{(k)}, t - \tau_l^{(k)} - sT)\, dt. \quad \text{(A6)}$$

Expanding,

$$I = A \int_0^T \tilde{X}_1^*\left(V_\lambda^{(1)}, t - \frac{p}{W}\right) \sum_{s=-\infty}^{\infty} \tilde{X}_k(V_\nu^{(k)}, t - \tau_l^{(k)} - sT)\, dt \quad \text{(A7)}$$

$$I = A \int_0^T \sum_{n=0}^{N-1} V_{\lambda,n}^{(1)^*} P_{T_c}\left(t - nT_c - \frac{p}{W}\right) \cdot \sum_{s=-\infty}^{\infty} \sum_{m=0}^{N-1} V_{\nu,m}^{(k)} P_{T_c}(t - mT_c - \tau_l^{(k)} - \Delta_k - sT)\, dt \quad \text{(A8)}$$

let $u = n - m$ and

$$\begin{aligned} y &= t - mT_c - \Delta_k - sT - \tau_l^{(k)} \\ &= t - (m + sN)T_c - \Delta_k - \tau_l^{(k)} \end{aligned} \quad \text{(A9)}$$

then, for $P_{T_c}(t)$ a rectangular pulse

$$I = A \sum_{m=0}^{N-1-u} V_{\nu,m}^{(k)} V_{\lambda,m+u}^{(1)^*} \int_0^T \sum_{s=-\infty}^{\infty} P_{T_c} \cdot \left(y - uT_c + \tau_l^{(k)} - \frac{p}{W} + \Delta_k + sT\right) P_{T_c}(y)\, dy. \quad \text{(A10)}$$

For $P_{T_c}(t)$ a rectangular pulse,

$$P_{T_c}(t) = \begin{cases} 1; & 0 \le t < T_c \\ 0; & \text{elsewhere} \end{cases} \quad \text{(A11)}$$

then

$$\int_0^{T_c} P_{T_c}(t) P_{T_c}(t - x)\, dt \begin{cases} = 0; & |x| \ge T_c \\ \ne 0; & -T_c < x < T_c \end{cases}. \quad \text{(A12)}$$

Therefore, for $I \ne 0$,

$$-T_c < \tau_l^{(k)} - \frac{p}{W} + \Delta_k + sT - uT_c < T_c \quad \text{(A13)}$$

Recall $T = N \cdot T_c$ so that

$$(u - sN - 1)T_c < \tau_l^{(k)} - \frac{p}{W} + \Delta_k < (u - sN + 1)T_c \quad \text{(A14)}$$

let

$$x = \tau_l^{(k)} - \frac{p}{W} + \Delta_k. \tag{A15}$$

If $x \geq 0$, then the following condition must be met:

$$0 \leq x < T_c \tag{A16}$$

or

$$(u - sN)T_c < \tau_l^{(k)} - \frac{p}{W} + \Delta_k < (u - sN + 1)T_c. \tag{A17}$$

Let $d = u - sN$

$$dT_c < \tau_l^{(k)} - \frac{p}{W} + \Delta_k < (d+1)T_c. \tag{A18}$$

For $x < 0$,

$$(d-1)T_c < \tau_l^{(k)} - \frac{p}{W} + \Delta_k < dT_c. \tag{A19}$$

Therefore, I can be expressed as

$$I = AR_{\nu,\lambda}^{(k,1)}\left(\tau_l^{(k)} - \frac{p}{W} + \Delta_k\right) \tag{A20}$$

where $R_{\nu,\lambda}^{(k,1)}$ is defined in Appendix B. The decision variable can now be written as

$$Z_\lambda = \mathrm{Re}\left\{A\sum_{p=0}^{P-1} a_p \exp(-j\varphi_p)\sum_{k=0}^{K-1}\sum_{l=0}^{L_k-1}\alpha_l^{(k)} \cdot \exp(j\phi_l^{(k)})R_{\nu,\lambda}^{(k,1)}\left(\tau_l^{(k)} - \frac{p}{W} + \Delta_k\right)\right\} + \eta_\lambda. \tag{A21}$$

The tap gains are computed as follows:

$$\begin{aligned} a_p \exp(+j\varphi_p) &= E\left\{\sum_{l=0}^{L_1-1}\alpha_l^{(1)}\exp(j\phi_l^{(1)})\int_0^T \tilde{X}_1^* \cdot \left(V_\lambda^{(1)}, t - \frac{p}{W}\right)X\left(t - \tau_l^{(1)}\right)dt\right\} \\ &= E\left\{\sum_{l=0}^{L_1-1}\alpha_l^{(1)}\exp(j\phi_l^{(1)})R_{\lambda,\lambda}^{(1,1)}\left(\tau_l^{(1)} - \frac{p}{W}\right)\right\} \\ &= \sum_{l=0}^{L_1-1}\alpha_l^{(1)}\exp(j\phi_l^{(1)})E\left\{R_{\lambda,\lambda}^{(1,1)}\left(\tau_l^{(1)} - \frac{p}{W}\right)\right\}. \end{aligned} \tag{A22}$$

The difference between decision variables for the first user is

$$Z_\zeta - Z_\lambda = \mathrm{Re}\left\{A\sum_{p=0}^{P-1} a_p \exp(-j\varphi_p)\sum_{k=0}^{K-1}\sum_{l=0}^{L_k-1}\alpha_l^{(k)} \cdot \exp(j\phi_l^{(k)})\left[R_{\nu,\zeta}^{(k,1)}\left(\tau_l^{(k)} - \frac{p}{W} + \Delta_k\right) - R_{\nu,\lambda}^{(k,1)}\left(\tau_l^{(k)} - \frac{p}{W} + \Delta_k\right)\right]\right\} + \eta_\zeta - \eta_\lambda. \tag{A23}$$

Assuming the statistics of the difference between decision variables follow a Gaussian distribution, the codes are random and orthogonal [9], and the λ th symbol is transmitted,

$$\begin{aligned} E\{Z_\zeta - Z_\lambda\} &= \mathrm{Re}\left\{-A\sum_{p=0}^{P-1} a_p \exp(-j\varphi_p)\sum_{l=0}^{L_1-1}\alpha_l^{(1)} \cdot \exp(j\phi_l^{(1)})R_{\lambda,\lambda}^{(1,1)}\left(\tau_l^{(1)} - \frac{p}{W}\right)\right\} \\ &= -A\sum_{p=0}^{P-1}\sum_{l=0}^{L_1-1} a_p\alpha_l^{(1)} \cdot \cos(\phi_l^{(1)} - \varphi_p)R_{\lambda,\lambda}^{(1,1)}\left(\tau_l^{(1)} - \frac{p}{W}\right) \end{aligned} \tag{A24}$$

$$\begin{aligned} &\mathrm{Var}\{Z_\zeta - Z_\lambda\} \\ &= A^2\sum_{p=0}^{P-1}\sum_{l=0}^{L_1-1}[a_p\alpha_l^{(1)}\cos(\phi_l^{(1)} - \varphi_p)]^2 \cdot Y_a\left(\tau_l^{(1)} - \frac{p}{W}\right) \\ &\quad + A^2\sum_{p=0}^{P-1}\sum_{k=1}^{K-1}\sum_{l=0}^{L-1}[a_p\alpha_l^{(k)}\cos(\phi_l^{(k)} - \varphi_p)]^2 \cdot Y_b\left(\tau_l^{(k)} - \frac{p}{W}\right) + N_0NT_c\sum_{p=0}^{P-1}|a_p|^2. \end{aligned} \tag{A25}$$

Therefore, the signal-to-noise ratio (SNR) for the RAKE receiver is

$$\gamma_{\mathrm{RAKE}} = \frac{\left[\sum_{p=0}^{P-1}\sum_{l=0}^{L_1-1} a_p\alpha_l^{(1)}\cos(\phi_l^{(1)} - \varphi_p)\, R_{\lambda,\lambda}^{(1,1)}\left(\tau_l^{(1)} - \frac{p}{W}\right)\right]^2}{N_{SI} + N_{MI} + N_I} \tag{A26}$$

where

$$N_{SI} = \sum_{p=0}^{P-1}\sum_{l=0}^{L_1-1}[a_p\alpha_l^{(1)}\cos(\phi_l^{(1)} - \varphi_p)]^2 Y_a\left(\tau_l^{(1)} - \frac{p}{W}\right) \tag{A27}$$

$$N_{MI} = \sum_{p=0}^{P-1}\sum_{k=1}^{K-1}\sum_{l=0}^{L_k-1}[a_p\alpha_l^{(k)}\cos(\phi_l^{(k)} - \varphi_p)]^2 Y_b\left(\tau_l^{(k)} - \frac{p}{W}\right) \tag{A28}$$

$$N_I = \frac{N_0}{E_b}\frac{(NT_c)^2}{2\log_2 M}\sum_{p=0}^{P-1}|a_p|^2 \tag{A29}$$

where $Y_a(\cdot)$ and $Y_b(\cdot)$ are defined in Appendix B. N_{SI} is the self-interference of the first user, N_{MI} is the mutual interference from the $K-1$ other users, and N_I is the noise.

Appendix B

The aperiodic auto- and cross-correlation function of the pseudonoise sequence vectors are defined as:

$$C(V_\nu^{(k)}, V_\lambda^{(1)})(l) = \begin{cases} \sum_{n=0}^{N-1-l} V_{\nu,n}^{(k)} V_{\lambda,n+l}^{(1)*}; & 0 \le l \le N-1 \\ \sum_{n=0}^{N-1+l} V_{\nu,n-l}^{(k)} V_{\lambda,n}^{(l)*}; & 1-N \le l < 0 \\ 0 & |l| \ge N \end{cases} \quad \text{(B1)}$$

where l is an integer. The phase of $V_{\lambda,n}^{(k)}$ is approximated by a uniform continuous distribution on $[0, 2\pi)$. For random sets of orthogonal codes, the first and second moments of the aperiodic auto- and cross-correlation functions are:

$$E\{C(V_\nu^{(k)}, V_\lambda^{(1)})(l)\} = \begin{cases} N; & k=1,\ \nu=\lambda,\ l=0 \\ 0; & \text{otherwise} \end{cases} \quad \text{(B2)}$$

$$E\{|C(V_\nu^{(k)}, V_\lambda^{(1)})(l)|^2\} = \begin{cases} N^2; & k=1,\ \nu=\lambda,\ l=0 \\ N-|l|; & k=1,\ 0<|l|\le N-1 \\ N-|l|; & k\ne 1,\ 0\le|l|\le N-1 \\ 0; & \text{otherwise} \end{cases} \quad \text{(B3)}$$

For the chip waveform:

$$H_p(s) = \int_0^s P_{T_c}(t) P_{T_c}(t+T_c-s)\,dt$$
$$\hat{H}_p(s) = \int_s^{T_c} P_{T_c}(t) P_{T_c}(t-s)\,dt \quad \text{(B4)}$$

For P_{T_c}, a rectangular pulse and $0 \le s < T_c$:

$$H_p(s) = s; \quad \hat{H}_p(s) = T_c - s. \quad \text{(B5)}$$

Then, if $dT_c \le \tau_l + \Delta_k < (d+1)T_c$, Δ_k for $k \ne 0$ uniformly distributed in $[0, T_c)$ and $\Delta_0 = 0$:

$$E\{\Delta_k\} = \frac{T_c}{2}; \qquad k \ne 0$$
$$E\{(\Delta_k)^2\} = \frac{T_c^2}{3}; \qquad k \ne 0 \quad \text{(B6)}$$

Then

$$\begin{aligned} R_{\lambda,\lambda}^{(1,1)}(\tau_l^{(1)}) &= H_p(\tau_l^{(1)} - dT_c) \\ &\quad \cdot [C(V_\nu^{(1)}, V_\lambda^{(1)})(d-N+1) + C(V_\lambda^{(1)}, V_\lambda^{(1)})(d+1)] \\ &\quad + \hat{H}_p(\tau_l^{(1)} - dT_c) \\ &\quad \cdot [C(V_\nu^{(1)}, V_\lambda^{(1)})(d-N) + C(V_\lambda^{(1)}, V_\lambda^{(1)})(d)] \end{aligned} \quad \text{(B7)}$$

$$\begin{aligned} R_{\nu,\lambda}^{(k,1)}(\tau_l^{(k)}) &= H_p(\tau_l^{(k)} - dT_c) \\ &\quad \cdot [C(V_\xi^{(k)}, V_\lambda^{(1)})(d-N+1) + C(V_\nu^{(k)}, V_\lambda^{(1)})(d+1)] \\ &\quad + \hat{H}_p(\tau_l^{(k)} - dT_c) \\ &\quad \cdot [C(V_\xi^{(k)}, V_\lambda^{(1)})(d-N) + C(V_\nu^{(k)}, V_\lambda^{(1)})(d)] \end{aligned} \quad \text{(B8)}$$

$$\begin{aligned} R_{\lambda,\nu}^{(1,1)}(\tau_l^{(1)}) &= H_p(\tau_l^{(1)} - dT_c) \\ &\quad \cdot [C(V_\xi^{(1)}, V_\nu^{(1)})(d-N+1) + C(V_\lambda^{(1)}, V_\nu^{(1)})(d+1)] \\ &\quad + \hat{H}_p(\tau_l^{(1)} - dT_c) \\ &\quad \cdot [C(V_\xi^{(1)}, V_\nu^{(1)})(d-N) + C(V_\lambda^{(1)}, V_\nu^{(1)})(d)] \end{aligned} \quad \text{(B9)}$$

$$\begin{aligned} R_{\xi,\nu}^{(k,1)}(\tau_l^{(k)}) &= H_p(\tau_l^{(k)} - dT_c) \\ &\quad \cdot [C(V_\mu^{(k)}, V_\nu^{(1)})(d-N+1) + C(V_\xi^{(k)}, V_\nu^{(1)})(d+1)] \\ &\quad + \hat{H}_p(\tau_l^{(k)} - dT_c) \\ &\quad \cdot [C(V_\mu^{(k)}, V_\nu^{(1)})(d-N) + C(V_\xi^{(k)}, V_\nu^{(1)})(d)] \end{aligned} \quad \text{(B10)}$$

Evaluating the statistics of the difference of the correlation terms;

$$\begin{aligned} E\{R_{\lambda,\nu}^{(1,1)}(\tau_l^{(1)}) - R_{\lambda,\lambda}^{(1,1)}(\tau_l^{(1)})\} &= -R_{\lambda,\lambda}^{(1,1)}(\tau_l^{(1)}) \\ &= \begin{cases} -N(T_c - \tau_l^{(1)}); & d=0 \\ -N\tau_l^{(1)}; & d=-1 \\ 0; & \text{elsewhere} \end{cases} \end{aligned} \quad \text{(B11)}$$

$$\begin{aligned} Y_a(\tau_l^{(1)}) &= \text{Var}\{R_{\lambda,\nu}^{(1,1)}(\tau_l^{(1)}) - R_{\lambda,\lambda}^{(1,1)}(\tau_l^{(1)})\} \\ &= H_p^2(\tau_l^{(1)} - dT_c) \\ &\quad \cdot (2\mathcal{E}_c(d-N+1) + \mathcal{E}_c(d+1) + \mathcal{E}_a(d+1)) \\ &\quad + \hat{H}_p^2(\tau_l^{(1)} - dT_c) \\ &\quad \cdot (\mathcal{E}_c(d) + 2\mathcal{E}_c(d-N) + \mathcal{E}_a(d)) \end{aligned} \quad \text{(B12)}$$

and, for $\Delta_k\,(k \ne 0)$ uniformly distributed in $[0, T_c)$ see (B13)–(B17) that follows.

$$E\{R_{\beta,\nu}^{(k,1)}(\tau_l^{(k)} + \Delta_k) - R_{\nu,\lambda}^{(k,1)}(\tau_l^{(k)} + \Delta_k)\} = 0 \quad \text{(B13)}$$

$$\begin{aligned} Y_b(\tau_l^{(k)}) &= \text{Var}\{R_{\beta,\nu}^{(k,1)}(\tau_l^{(k)} + \Delta_k) - R_{\nu,\lambda}^{(k,1)}(\tau_l^{(k)} + \Delta_k)\} \\ &= 2[\mathcal{E}_b(d+1) + \mathcal{E}_b(d-N+1)] \\ &\quad \cdot \left[(\tau_l^{(k)} - dT_c)^2 + T_c\left(\frac{T_c}{3} + \tau_l^{(k)} - dT_c\right)\right] \\ &\quad + 2[\mathcal{E}_b(d) + \mathcal{E}_b(d-N)] \\ &\quad \cdot \left[((1+d)T_c - \tau_l^{(k)})^2 + T_c\left(\frac{T_c}{3} + \tau_l^{(k)} - (1+d)T_c\right)\right] \end{aligned} \quad \text{(B14)}$$

where

$$\mathcal{E}_a(l) = \text{Var}\{C(V_\lambda^{(1)}, V_\lambda^{(1)})(l)\} = \begin{cases} N-|l|; & 0<|l|\le N-1 \\ 0; & \text{otherwise} \end{cases} \quad \text{(B15)}$$

$$\mathcal{E}_b(l) = \text{Var}\{C(V_\nu^{(k)}, V_\lambda^{(1)})(l)\} = \begin{cases} N-|l|; & 0\le|l|\le N-1 \\ 0; & \text{otherwise} \end{cases} \quad \text{(B16)}$$

$$\mathcal{E}_c(l) = \text{Var}\{C(V_\nu^{(1)}, V_\lambda^{(1)})(l)\} = \begin{cases} N-|l|; & 0<|l|\le N-1 \\ 0; & \text{otherwise} \end{cases} \quad \text{(B17)}$$

REFERENCES

[1] K. Pahlavan, "Wireless communications for office information networks," *IEEE Commun. Mag.*, vol. 23, pp. 19–27, June 1985.

[2] P. Ferert, "Application of spread-spectrum radio to wireless terminal communications," in *Proc. IEEE Nat. Telecommun. Conf.*, Dec. 1980, pp. 244–248.

[3] M. J. Marcus, "Recent U.S. regulatory decisions on civil use of spread spectrum," in *Proc. IEEE GLOBECOM*, Dec. 1985, pp. 16.6.1–16.6.3.

[4] K. Pahlavan, "Wireless intra-office networks," *ACM Trans. Office Inform. Networks*, July 1988.

[5] M. Kavehrad and P. J. McLane, "Performance of low-complexity channel coding and diversity for spread spectrum in indoor wireless communications," *AT&T Tech. J.*, vol. 64, no. 8, pp. 1927–1965, Oct. 1985.

[6] M. Kavehrad and B. Ramamurthi, "Direct sequence spread spectrum with DPSK modulation and diversity for indoor wireless communications," *IEEE Trans. Commun.*, vol. COM-35, pp. 224–236, Feb. 1987.

[7] M. Chase and K. Pahlavan, "Spread spectrum multiple-access performance of orthogonal codes in fading multipath channels," *IEEE MILCOM*, Oct. 1988, pp. 5.4.1–5.4.5.

[8] J. S. Lehnert and M. B. Pursley, "Multipath diversity reception of spread-spectrum multiple-access communications," *IEEE Trans. Commun.*, vol. COM-35, pp. 1189–1198, Nov. 1987.

[9] P. K. Enge and D. V. Sarwate, "Spread spectrum multiple-access performance of orthogonal codes: linear receivers," *IEEE Trans. Commun.*, vol. COM-35, pp. 1309–1319, Dec. 1987.

[10] K. Pahlavan and M. Chase, "Spread-spectrum multiple-access performance of orthogonal codes for indoor radio communications," *IEEE Trans. Commun.*, vol. 38, pp. 574–577, May 1990.

[11] R. Ganesh and K. Pahlavan, "On the modeling of the fading multipath indoor radio channel," *IEEE GLOBECOM*, 1989.

[12] J. G. Proakis, *Digital Communications.* New York: McGraw-Hill, 1989.

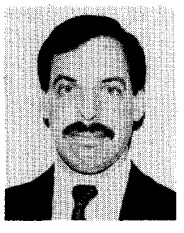

Mitchell Chase (S'73–M'78) was born in Brooklyn, New York on October 10, 1951. He received the B.E. degree in electrical engineering from the City College of New York, New York City, in 1974, the M.S. degree in biomedical engineering from Iowa State University, Ames, IA, in 1976, the M.B.A. degree from Northeastern University, Boston, MA, in 1982, and the Ph.D. degree in electrical engineering from Worcester Polytechnic Institute, Worcester, MA, in 1993.

Since 1978 he has held a variety of positions at several companies developing products ranging from agricultural electronics to flight simulators and automated systems for the identification of blood cells. He is currently an Applications Engineer with Comdisco Systems, Inc. His current research interests are in the areas of spread spectrum and wireless communications. He has authored several publications in this area as well as in the areas of digital and image signal processing, graphics, and biomedical engineering.

Kaveh Pahlavan is a Professor of Electrical and Computer Engineering and the Director of the Center for Wireless Information Network Studies at the Worcester Polytechnic Institute, Worcester, MA. His basic research in the past few yers has been focused on indoor radio propagation modeling and analysis of the multiple access and transmission methods for wireless local networks. His previous research background is on modulation, coding, and adaptive signal processing for digital communication over voice-band and fading multipath radio channels. He has contributed to numerous technical papers, has presented many tutorials and short courses in various countries and has been a consultant to many industries including CNR Inc., GTE Laboratories, Steinbrecher Corporation, Simplex Company, and WINDATA Inc. Before joining WPI, he was the Director of Advanced Development at Infinite Inc., Andover, MA, working on voice band data communications. He started his career as an Assistant Professor at Northeastern University, Boston, MA. He is the Editor-in-Chief of the *International Journal on Wireless Information Networks*. He was the program chairman and organizer of the IEEE Wireless LAN Workshop, Worcester, MA, May 9, 10, 1991 and the organizer and the technical program chairman of the 3rd IEEE International Symposium on Personal, Indoor, and Mobile Radio Communications, Boston, MA, October 19–21, 1992. He is a Member of Eta Kappa Nu and a Senior Member of the IEEE Communication Society.

BER Performance of Anti-Multipath Modulation Scheme PSK-VP and its Optimum Phase-Waveform

Hitoshi Takai, *Member, IEEE*

Abstract—**This paper proposes a new anti-multipath modulation scheme, which the author calls PSK-VP (phase-shift-keying with varied phase), in which a time-varying phase-waveform is redundantly imposed on the DPSK timeslot. The relationship between the phase-waveform and BER (bit-error rate) is discussed by using an analytical approach which considers the diversity of received signal components that are continuously varying over a symbol period. A formula-type BER expression obtained by this analytical approach yields a maximum-diversity phase-waveform condition. A convex phase-waveform is considered to be the best choice because of this condition and an additional consideration for spectrum compactness. A numerical evaluation confirms the performance of *PSK-VP with a convex phase-waveform* and reveals a band-limitation effect. From the numerical evaluation, it is shown that the 4-ary version of PSK-VP with a convex phase-waveform has an excellent BER performance in multipath fading when the delay dissipation is less than 1.7 bits, although requiring about twice the bandwidth due to the imposed phase redundancy.**

I. Introduction

HIGH-SPEED digital mobile communications are severely affected by the frequency-selective fading caused by multipath with various time delays [1], [2], which characterizes their radio channels. Severe intersymbol interference caused by the frequency-selective fading greatly degrades the BER (bit error rate) [3], and consequently limits the maximum transmission data rate.

To combat the BER degradation, various anti-multipath modulation schemes, in which a redundant phase/amplitude transition is imposed on a basic conventional modulation, have been proposed [4]–[8]. In a DSK [4] scheme, a phase-jump, the direction of which has the same binary information as symmetric BPSK, is repeated twice for every information bit. In an SPSK [7] scheme, a phase-jump is redundantly imposed on the DPSK timeslot. MC-PSK [8] is a specific case of SPSK, which has a redundant π-phase-jump at the center of the timeslot. In a PSK-RZ [5], [6] scheme, an amplitude quench is redundantly imposed on the latter half of the DPSK timeslot.

In these modulation schemes, by means of the imposed phase/amplitude transition, different kinds of effective detected signal components, of which polarity is always correct with respect to the transmitted data, are obtained in a differential detector output for a multipath fading channel. Here, "different kinds" means that the individual detected signal components change differently with the variations of the fading of the channel. Specifically, each detected signal component may become small or disappear at times; however, it is rare for all of the detected signal components to disappear simultaneously. Therefore, by also using a postdetection filter to combine the detected signal components, diversity effect is expected.[1]

In general, anti-multipath modulation schemes are characterized by *hardware simplicity,* because no adaptive process is required, and by their *excellent BER's* due to the above diversity effect in multipath fading, when the delay dispersion is less than a certain value (hereafter referred to as *delay dispersion upper limit*). The variety of the effective detected signal components, or the existence condition of that variety, which determines the delay dispersion upper limit, differs among the individual modulation schemes. Therefore, there are differences among these modulation schemes in BER performance, particularly with respect to the delay dispersion upper limit, as well as the required bandwidth.

Raising the delay dispersion upper limit, which is equivalent to raising the usable bit rate, is an important problem for such anti-multipath modulation schemes, because the limit is rather low for applications to various propagation environments or applications at a higher bit rate. The choice of the basic modulation and how the redundancy should be imposed determine the upper limit. By choosing DPSK as the basic modulation, PSK-RZ [5], [6] with amplitude redundancy, SPSK [7] and MC-PSK [8] with redundant phase-jump extend the limit. This is because M-ary versions of the above can significantly extend the limit as measured in bits. Concurrently, the M-ary versions are also advantageous in spectrum compactness. However, optimization for redundancy to extend the limit has not been discussed.

In this paper, it through an investigation of the phase-redundancy optimization, the author proposes *PSK-VP with a convex phase-waveform* as an answer to the problem. As will be shown in Section II, PSK-VP (phase shift keying with varied phase) [10] is defined as a generic name for modulation schemes in which a *time-varying phase-waveform* is redundantly imposed on the DPSK timeslot. Then, optimum shape of the redundant phase-waveform is discussed.

PSK-VP is characterized using an analytical approach and a numerical evaluation. The analytical approach reveals its BER

Manuscript received April, 1991; revised June 6, 1991, and September 18, 1992.

The author was with ATR Optical and Radio Communications Research Laboratories, Seika-cho, Soraku-gun, Kyoto 619-02, Japan. He is now with the Communication Systems Research Laboratory, Matsushita Electric Industrial Co., Ltd., Osaka 571, Japan.

IEEE Log Number 9207440.

[1] TFSK [9] scheme has a similar concept to the anti-multipath modulation in that a redundant phase-hold is imposed on the MSK timeslot. However, in TFSK, the diversity effect cannot be expected because only one kind of effective detected signal component is obtained.